Perturbation of higher-order solitons by fourth-order dispersion in optical fibers

Samudra Roy [a], Shyamal K. Bhadra [a,*], Govind P. Agrawal [b]

[a] *Fiber Optics Laboratory, Central Glass and Ceramic Research Institute, CSIR 196 Raja S.C. Mullick Road, Kolkata 700032, India*
[b] *Institute of Optics, University of Rochester, Rochester, NY 14627, USA*

ABSTRACT

We study analytically and numerically how the radiation emitted by fundamental solitons in the form of dispersive waves is affected by the third and fourth-order dispersions when a higher-order soliton undergoes the fission process inside an optical fiber. Our results show that two dispersive wave sidebands appear in the output spectrum on opposite sides of the input spectrum. The frequencies of these sidebands are set by the relative magnitudes of the third- and fourth-order dispersion parameters, but are not affected much by the Raman process. A well defined phase-matching condition accurately predicts these conjugate frequencies of dispersive wave. The relative amplitudes of these two sidebands are not equal because of the asymmetry induced by the third-order dispersion and higher-order nonlinearities. It is found that with increasing fourth-order dispersion the amplitude of both spectral components eventually saturate and the relative power level associated with one of the components can exceed 10% of the launched power under suitable conditions. This component is the one that will form even in the absence of fourth-order dispersion and its wavelength may lie on the red or the blue side of the launched wavelength depending on the sign of the dispersion slope at this wavelength. It is also observed that soliton order itself significantly influence the peak amplitude of the radiation and play a minor role in determining radiation frequencies. We believe, these results should be of relevance for applications requiring an ultrabroadband optical source and understanding the interesting facts of supercontinuum generation.

© 2009 Elsevier B.V. All rights reserved.

1. Introduction

It is well known that, under ideal conditions, higher-order solitons forming inside optical fibers exhibit periodic evolution such that the optical pulse recovers its input shape after a distance known as the soliton period [1–3]. Such a stable propagation of higher-order optical soliton ceases to occur in the presence of higher-order dispersive effects. Typically, a higher-order soliton disintegrates into its constituent fundamental solitons in the presence of such perturbations, a phenomenon referred to as the soliton-fission [2]. The inverse scattering method shows that the power and width of the kth soliton are related to the soliton order N as [1,2], $P_k = P_0(2N + 1 - 2k)^2/N^2$ and $T_k = T_0/(2N + 1 - 2k)$, where P_0 and T_0 are the input power and pulse width, respectively. The most energetic soliton ($k = 1$), which has the shortest temporal width, is termed the Raman soliton, and it is primarily responsible for the non-solitonic radiation (NSR). Right after the fission process, higher-order dispersive effects transfer a part of the soliton energy in the form of a dispersive wave (DW) at a specific frequency set by the phase-matching condition [4]. The emission of NSR in the form of dispersive waves is of particular importance for supercontinuum generation [5–9]. After an early numerical work in 1986 identified

the NSR [4], a considerable research activity has established the essential role played by the third-order dispersion (TOD) in generating the NSR [10–14]. Although it was pointed out in a 1995 study that the fourth-order dispersion (FOD) should generate two NSR peaks on the red and blue sides of the original pulse spectrum [13], except for a recent experimental confirmation [15], little attention has been paid to the role of FOD in forming the supercontinuum inside optical fibers.

At this point, it should be mentioned that the appearance of two zero-dispersion wavelengths (ZDW) in some fibers is connected with the dominance of FOD term that leads to the conjugate radiations on both side of the input spectrum. Properly designed microstructured fibers may possess this special dispersion characteristic. Soliton spectral tunneling (SST) is another interesting phenomenon [16,17] that occurs with this kind of dispersion behavior when two anomalous dispersion regions are separated by an intermediate normal-dispersion zone. Physically, a soliton formed in one anomalous dispersion region transfers its energy to a linear wave at a resonance frequency near the other zero-dispersion point. This sharp switching of soliton frequency from one anomalous dispersion domain to the other is interpreted by analogy with quantum mechanical tunneling through a potential barrier [18]. Apart from the SST effect, supercontinuum (SC) generation in a photonic crystal fiber (PCF) with two ZDWs has been studied extensively in [19–21], where

* Corresponding author.
  E-mail address: skbhadra@cgcri.res.in (S.K. Bhadra).

issues related to dual pumping [19], soliton-pair generation [20], etc., are considered but not explicitly the issues related to DW generation.

In this work, we focus on a systematic study of the growth of dual-frequency NSR as recently observed [15,21]. We concentrate on the role of FOD which is primarily responsible for the simultaneous generation of two DWs. Of course, we should not consider FOD without including TOD because, in most practical cases, both types of dispersions are present simultaneously. Moreover, we should also include a higher-order nonlinear effect known as intrapulse Raman scattering (IPRS) [3] because it is essential for supercontinuum generation [9]. With this in mind, we study numerically the propagation of higher-order solitons inside optical fibers under the combined influence of FOD, TOD, and IPRS. We also generalize the analysis of Akhmediev and Karlsson [13] for the case of higher-order solitons and derive analytical expressions for the frequencies of the NSR peaks in the output spectrum due to the combined influence of FOD and TOD. Starting from a simple propagation equation we eventually solve the most general nonlinear Schrödinger equation in order to capture the role of all higher-order dispersion and nonlinear terms in generating dispersive waves. The study reveals a clear picture of the growth of dispersive waves during SC generation process. The frequencies of the radiation is obtained by the phase-matching condition in the form of a polynomial whose coefficients depend on the numerical values of properly normalized third and higher-order dispersion parameters. It is observed that amplitude and frequency of the dispersive wave critically depends on the relative values of dispersion coefficients. We perform extensive numerical simulations to verify the analytical prediction of radiation frequencies. The results reveal several valuable features related to the growth of NSR that should be of relevance for the study of supercontinuum.

2. Frequencies of two NSR peaks

As is known from previous work [13,14], it is much more useful to employ a normalized form of the nonlinear Schrödinger equation (NLSE) that makes use of the so-called soliton units. Since solitons require anomalous dispersion, we assume that the second-order dispersion parameter β_2 is negative at the carrier frequency ω_0 of the input pulse so that the pulse experiences anomalous dispersion inside the optical fiber. After including both the TOD and FOD terms, the normalized NLSE takes the following form [1],

$$i\frac{\partial U}{\partial \xi} + \frac{1}{2}\frac{\partial^2 U}{\partial \tau^2} + N^2|U|^2 U = i\delta_3 \frac{\partial^3 U}{\partial \tau^3} - \delta_4 \frac{\partial^4 U}{\partial \tau^4}, \tag{1}$$

where the field amplitude $U(\xi, \tau)$ is normalized such that $U(0, 0) = 1$ and the other dimensionless variables are defined as [1]

$$\xi = \frac{z}{L_D}, \ \tau = \frac{t - z/v_g}{T_0}, \ N = \sqrt{\gamma P_0 L_D}, \ \delta_3 = \frac{\beta_3}{6|\beta_2|T_0}, \ \delta_4 = \frac{\beta_4}{24|\beta_2|T_0^2}. \tag{2}$$

Here, T_0 and P_0 are related to the width and the peak power of the ultrashort pulse launched into the fiber, $L_D = T_0^2/|\beta_2|$ is the dispersion length, v_g is the group velocity, γ is nonlinear parameter, β_2 is the second-order dispersion parameter, and β_3 and β_4 are respectively the TOD and FOD coefficients of the fiber. The dimensionless quantity N is the soliton order defined such that $N = 1$ for a fundamental soliton [1]. In the absence of TOD ($\delta_3 = 0$) and FOD ($\delta_4 = 0$), Eq. (1) predicts that an input pulse, launched with the amplitude $U(0,\tau) = \text{sech}(\tau)$ and a peak power such that $N = 1$, propagates as the fundamental soliton with the general solution $U(\xi,\tau) = \text{sech}(\tau)\exp(i\xi/2)$. Such an input pulse maintains its shape and width

perfectly. This scenario ceases to occur when a fundamental soliton is perturbed by the TOD ($\delta_3 \neq 0$) or/and FOD ($\delta_4 \neq 0$) during its propagation inside the fiber.

In general, both terms on the right side of Eq. (1) act as a perturbation and generate NSR. From the previous study in Ref. [13] it is known that the NSR occurs at one specific frequency when δ_3 acts alone ($\delta_4 = 0$) and at two frequencies located symmetrically on the opposite side of ω_0 when δ_4 acts alone ($\delta_3 = 0$). We can use the same method to find the NSR frequencies when both the TOD and FOD terms are present simultaneously and a higher-order soliton is launched into the fiber. As it is already mentioned, the Nth-order soliton splits into N first-order solitons of different widths and peak powers through the fission process [2], and subsequently each fundamental soliton radiates a part of this energy to create the NSR at a few specific frequencies because of perturbations induced by TOD and FOD. Since the shortest soliton with a width $T_s = T_0/(2N - 1)$ is perturbed the most, we focus on this specific soliton in the following analysis. This soliton has a width T_s that is $(2N - 1)$ times smaller than the input pulse width T_0 and its peak power is larger by a factor of $(2N - 1)^2/N^2$ [2]. In our notation, the NSR frequencies are calculated by using the following phase-matching condition [13]:

$$\delta_4 f^4 + \delta_3 f^3 - \frac{1}{2}f^2 = \frac{1}{2}(2N - 1)^2, \tag{3}$$

where the normalized frequency f is given by $f = 2\pi(v_d - v_s)T_0$ and v_s and v_d are the carrier frequencies associated with the soliton and the dispersive wave, respectively. The quadratic polynomial in Eq. (3) has 4 solutions, not all of them may be real. It turns out that only two solutions are real in practice, indicating that NSR will lead to the formation of two NSR peaks located on opposite sides of the soliton frequency v_s.

3. Intrapulse Raman scattering (simple model)

In a simple model, the IPRS is included approximately by adding an additional term to the right side of Eq. (1). Resulting in the following modified NLSE [1]:

$$i\frac{\partial U}{\partial \xi} + \frac{1}{2}\frac{\partial^2 U}{\partial \tau^2} + N^2|U|^2 U = i\delta_3 \frac{\partial^3 U}{\partial \tau^3} - \delta_4 \frac{\partial^4 U}{\partial \tau^4} + i\tau_R \frac{\partial|U|^2}{\partial \tau}, \tag{4}$$

where $\tau_R = T_R/T_0$ and T_R is the IPRS coefficient with a value of about 3 fs. This model assumes that the pulse bandwidth is a small fraction of the Raman shift (about 13.2 THz for silica fibers) and is thus valid for pulses longer than 1 ps or so. The case of femtosecond pulses is discussed in the following section.

We used a standard split-step Fourier method [1] to solve Eq. (4) numerically. The results shown in Fig. 1 correspond to a total propagation distance of four dispersion lengths and assume that the input pulse is launched such that it propagates as a second-order soliton ($N = 2$). Fig. 1a shows the idealized situation in which only the FOD term acts as a perturbation ($\delta_4 = 0.001$), i.e., we set $\delta_3 = 0$ and $\tau_R = 0$. As expected from the theory given in Ref. [13], the FOD creates two spectral peaks located symmetrically on the red and blue side of the input carrier frequency. Fig. 1b shows how these NSR peaks are affected by the presence of TOD ($\delta_3 = 0.01$). As one would expect, the presence of TOD destroys the symmetric nature of the NSR peaks. At the same time, the amplitude of the blue peak increases while that of the red peak decreases. The frequency changes, induced by a finite value of the TOD parameter, are expected from the phase-matching condition given in Eq. (3). It should be noted that, being dimensionless quantities, one can get the same values of δ_3, δ_4, and N for many different combinations of the pulse parameters T_0 and P_0 and fiber parameters β_2, β_3, and β_4. Our results indicate that the resulting output spectrum will be
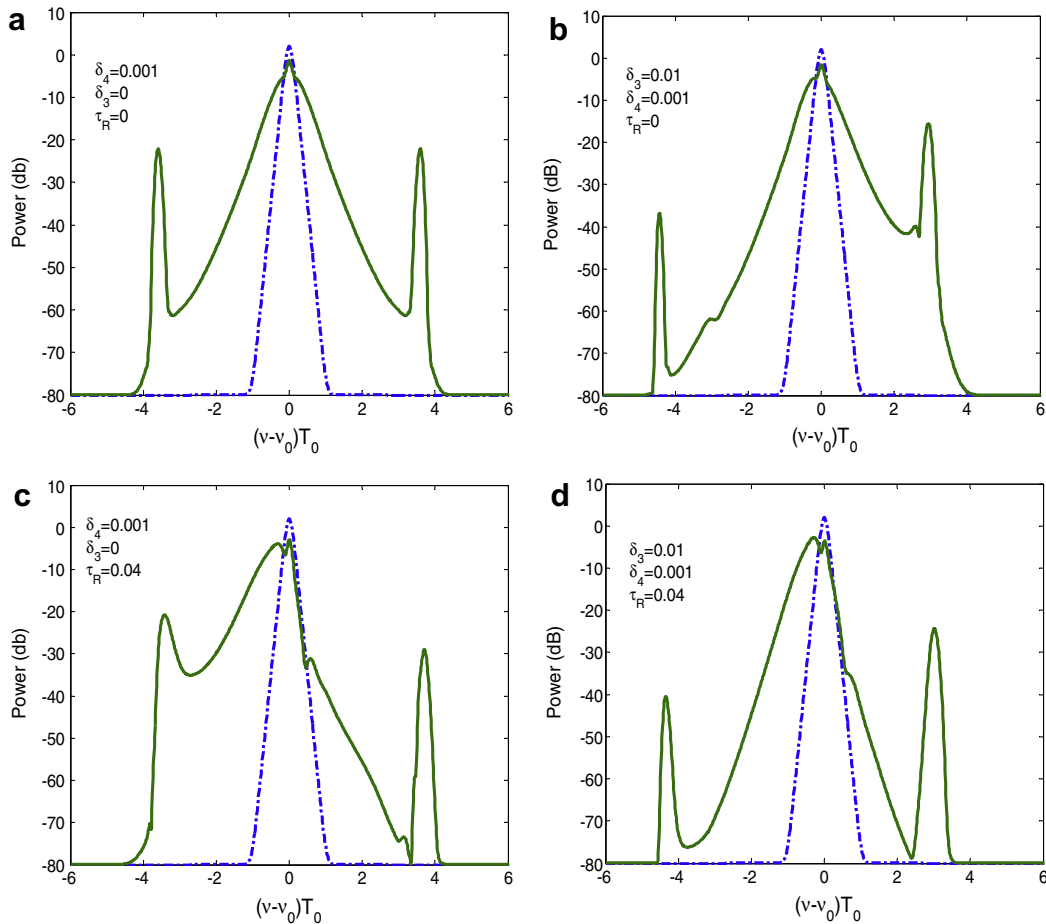
Fig. 1. Output spectra after four dispersion length for four different combinations of δ_3, δ_4 and τ_R. Input pulse excites a second-order soliton that splits into two fundamental solitons soon after the pulse is launched inside an optical fiber.

the same in all cases as long as the dimensionless parameters δ_3, δ_4, and N have the same values.

We study next how the amplitudes and the frequencies of the two NSR peaks are affected by the IPRS, a process that transfers part of the pulse energy toward longer wavelengths. Fig. 1c shows the influence of IPRS on the output pulse spectrum in the presence of FOD alone ($\delta_3 = 0$). As one may expect, the spectrum becomes asymmetric because of a continuous transfer of energy from high frequencies to low frequencies [3]. However, notice that neither the positions nor the amplitudes of the NSR peaks are affected much by the IPRS process. This feature indicates that the dispersive waves are generated right after the soliton-fission process and their frequencies and amplitudes are not affected by the subsequent energy transfer induced by IPRS. In Fig. 1d we include the effects of the TOD and IPRS effects simultaneously and obtain the output spectrum under a more general and realistic situation. The spectrum is changed significantly from that seen in Fig. 1c. In particular, we find that the blue side of the pulse spectrum contains more pulse energy compared with the red side. This is related to the fact that that TOD by itself creates an NSR peak on the blue side of the spectrum when $\delta_3 > 0$. Even though a single peak occurs on the blue side in the presence of both TOD and FOD, its amplitude is enhanced as both perturbations contribute to it. The results shown in Fig. 1 indicate that a symmetric NSR spectrum similar to that shown in plot (a) is unlikely to be observed because of the influence of TOD and IPRS both of which are likely to be present. Indeed, the blue NSR peak was found to be more intense than the red one in a recent experiment [15].

4. Intrapulse Raman scattering (comprehensive model)

The simple IPRS model based on Eq. (4) is reasonably accurate for picosecond pulses but should not be used for pulses whose widths are close to 100 fs or shorter. From the recent work on supercontinuum generation [9] it is known that the following generalized NLSE is quite adequate for numerical simulations under such conditions:

$$\frac{\partial U}{\partial \xi} = \frac{i}{2}\frac{\partial^2 U}{\partial \tau^2} + \delta_3 \frac{\partial^3 U}{\partial \tau^3} + i\delta_4 \frac{\partial^4 U}{\partial \tau^4}$$
$$+ iN^2\left(1 + is\frac{\partial}{\partial \tau}\right)\left(U(\xi,\tau)\int_{-\infty}^{\tau} R(\tau-\tau')|U(\xi,\tau')|^2 d\tau'\right). \quad (5)$$

Here, $s = (\omega_0 T_0)^{-1}$ is the self-steepening parameter and $R(\tau)$ is the nonlinear response function of an optical fiber in the form

$$R(\tau) = (1 - f_R)\delta(\tau) + f_R h_R(\tau), \quad (6)$$

where the first and the second terms correspond to the electronic and Raman responses, respectively. As discussed in Ref. [22], a suitable form of the Raman response function is of the form

$$h_R(\tau) = (f_a + f_c) h_a(\tau) + f_b h_b(\tau), \quad (7)$$

where the functions $h_a(\tau)$ and $h_b(\tau)$ are defined as

$$h_a(\tau) = \frac{\tau_1^2 + \tau_2^2}{\tau_1 \tau_2^2} \exp\left(-\frac{\tau}{\tau_2}\right)\sin\left(\frac{\tau}{\tau_1}\right),$$

$$h_b(\tau) = \left(\frac{2\tau_b - \tau}{\tau_b^2}\right)\exp\left(-\frac{\tau}{\tau_b}\right). \quad (8)$$

Various parameters governing the Raman response are obtained by fitting the experimentally observed Raman gain spectrum and are found to be $f_R = 0.245, f_a = 0.75, f_b = 0.21$, and $f_c = 0.04$. The three time intervals τ_1, τ_2 and τ_b have values of 12, 32 and 96 fs, respectively. In our notation, they have been normalized by the input pulse width T_0.

As before, we employ the standard split-step Fourier method [1] to solve Eq. (5) numerically for values of δ_4 in the range of 0.001– 0.01 at a set of fixed values of δ_3. The input "sech" pulses are assumed to have a carrier wavelength of 835 nm and a width such that $T_0 = 50$ fs (full width at half maximum of about 88 fs). Their peak power is chosen such that the soliton order N takes the value 2. In the following simulations, the fiber length corresponds to one dispersion length (ξ varies from 0 to 1). The physical fiber length depends on the value of β_2 and would be 2.5 m for $\beta_2 = 1$ ps²/ km. We stress that the self-steepening effects are negligible in our simulations because $s < 0.01$ for $T_0 = 50$ fs. Thus, IPRS is the major higher-order nonlinear process affecting the following numerical simulations performed by varying δ_4 in the range of 0.001–0.01. The phase-matching condition in Eq. (3) gives two real solutions in all cases investigated. The NSR wavelength falls on the red side ($\nu_d < \nu_s$) of the input spectrum for one of them and on the blue side ($\nu_d > \nu_s$) for the other one.

Fig. 2 shows the output pulse spectrum under for different dispersion conditions. The case $\delta_3 = 0$ (no TOD) shown in Fig. 2a applies to a special dispersion-flattened fiber in which the dispersion slope vanishes at the input wavelength of 835 nm. As before, the FOD creates two peaks on red and blue side of the input spectrum. The peak on the red side is more intense than the blue one because of the IPRS effects. A noteworthy feature is that both

the frequencies and amplitudes of the two NSR peaks change significantly with changes in the value of δ_4. More specifically, the two peaks move closer as δ_4 increases and their peak powers improve radically with increasing δ_4, reaching close to 10% of the input peak power for $\delta_4 = 0.004$. The addition of even a relatively small amount of TOD in Fig. 2b and c changes the spectrum significantly. The amplitude of the blue peak increases with increasing δ_3 and its frequency shifts toward the input frequency. In contrast, the red peak generated only by FOD, shifts more and more toward the red side and its amplitude decreases drastically.

The spectra shown in Fig. 2c for $\delta_3 = 0.02$ reveal the competition between the TOD and FOD effects. When δ_4 has a relatively small value of 0.001, the blue NSR peak dominates while the red peak has almost disappeared (its amplitude is below −85 dB), both features indicating that the TOD perturbation dominates compared with the FOD one. However, when δ_4 has a relatively large value of 0.005, the blue and red NSR peaks have large and comparable magnitudes, a feature indicating that the FOD perturbation dominates in this case. To provide further evidence of the competition between the TOD and FOD perturbations, we show in Fig. 2d the output spectra for three different values of δ_4 such that the ratio of δ_3 and δ_4 is fixed at 10. Under such conditions, both perturbations contribute to the NSR generation process such that the blue peak is stronger than the red one (because of the TOD effects). However, as δ_3 and δ_4 increase (with their ratio fixed at 10), the two peaks move closer and eventually begin to merge with the central part of the pulse spectrum.

Next, we investigate how well the analytical prediction for the frequencies of the NSR peaks based on Eq. (3) agrees with the full numerical solutions based on Eq. (5). Fig. 3a shows the predicted
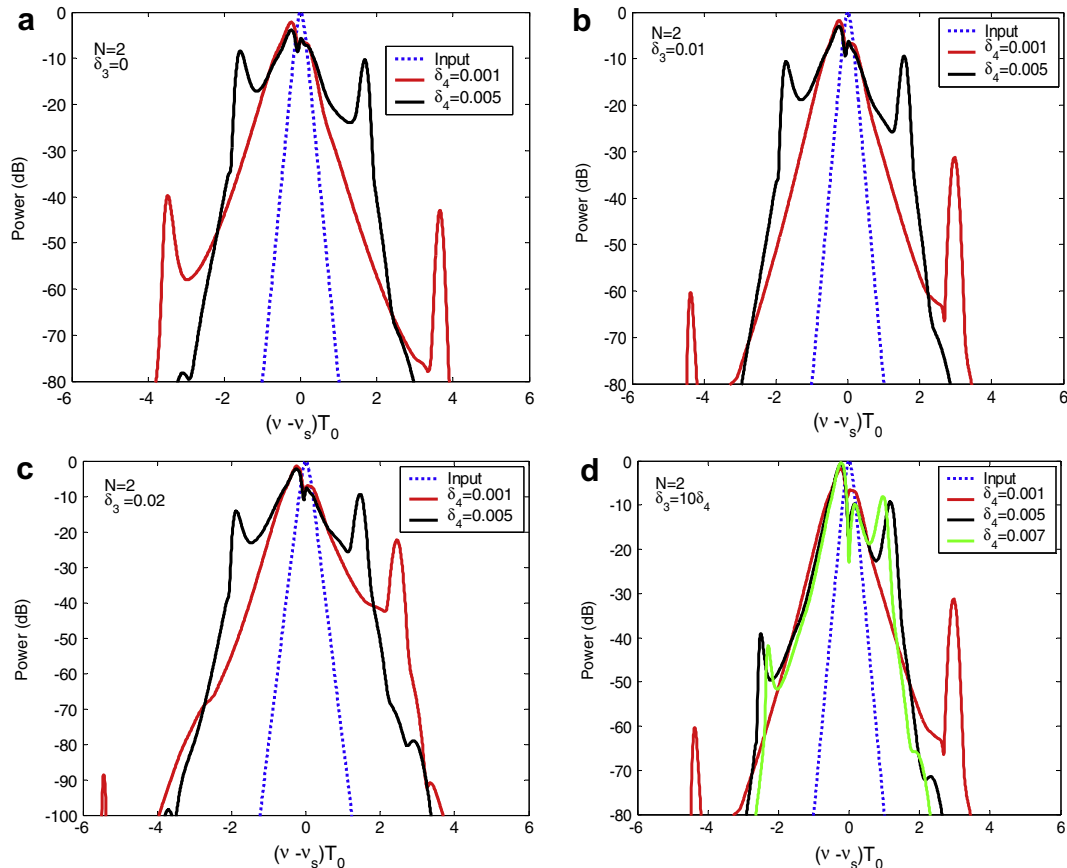
Fig. 2. Output spectra after one dispersion length for different combinations of δ_3 and δ_4. The generalized NLSE given in Eq. (5) is solved numerically for a femtosecond input pulse with $T_0 = 50$ fs.

and numerically calculated frequencies of the red and blue NSR peaks as a function of δ_4 for the second-order soliton ($N = 2$). We used three different values of δ_3 during the simulations ($\delta_3 = 0$, 0.01 and 0.02) for this comparison. Open circles represent the numerical values and the solid lines depict the corresponding analytical prediction obtained by solving the quadratic polynomial given in Eq. (3). The close agreement justifies the use of the phase-matching condition given in Eq. (3) and indicates that the IPRS process does not affect the NSR frequencies. The results also show that the NSR frequencies (both for the blue and red peaks) move closer with increasing values of δ_4 and their relative spacing eventually becomes constant. In the presence of TOD, the blue peak shifts towards the central frequency with increasing δ_3, while the red peak shifts away from the central frequency.

We also estimate numerically the peak power of the NSR peaks as a function of δ_4 for three different values of δ_3, and the results are shown in Fig. 3b. Both NSR peaks become more intense with increasing δ_4 and their power saturates eventually. The difference between the peak powers associated with the red and blue peaks becomes large for high value of δ_3. In particular, TOD reduces the amplitude of the red peak and enhances that of the blue peak. In

the absence of TOD [blue curves in Fig. 3b] the two peaks have almost the same power. A slight mismatch in powers occurring even in the $\delta_3 = 0$ case is due to the presence of IPRS.

So far we have discussed the growth of conjugate radiation peaks for a second-order soliton ($N = 2$). The phase-matching equation given in (3), in principle, holds for all higher-order solitons. For fixed values of δ_3 and δ_4 the radiation frequency changes only slightly with changing N. It is observed that the radiation peaks generated for $N = 2$ are smooth and distinctly positioned. This is the main reason for taking $N = 2$ in our simulations. These distinct peaks become distorted with increasing soliton order. In fact it is really hard to identify the exact location of the radiation peaks in spectral domain for $N > 4$. According to the observation of Cristiani et al. [7], dispersive radiation occurs at spectral expansion and each time the radiation frequency differ slightly from the previous one. This process eventually generates some extra fringes around the original radiation peak. Because of this, the DW peaks generated by the Raman soliton lose their identity with increasing soliton order, and measurements of the radiation frequency become erroneous. Here, we repeat the simulation for $N = 3$, and the results are shown in Fig. 4a. Even in this case, we find a reasonable agreement
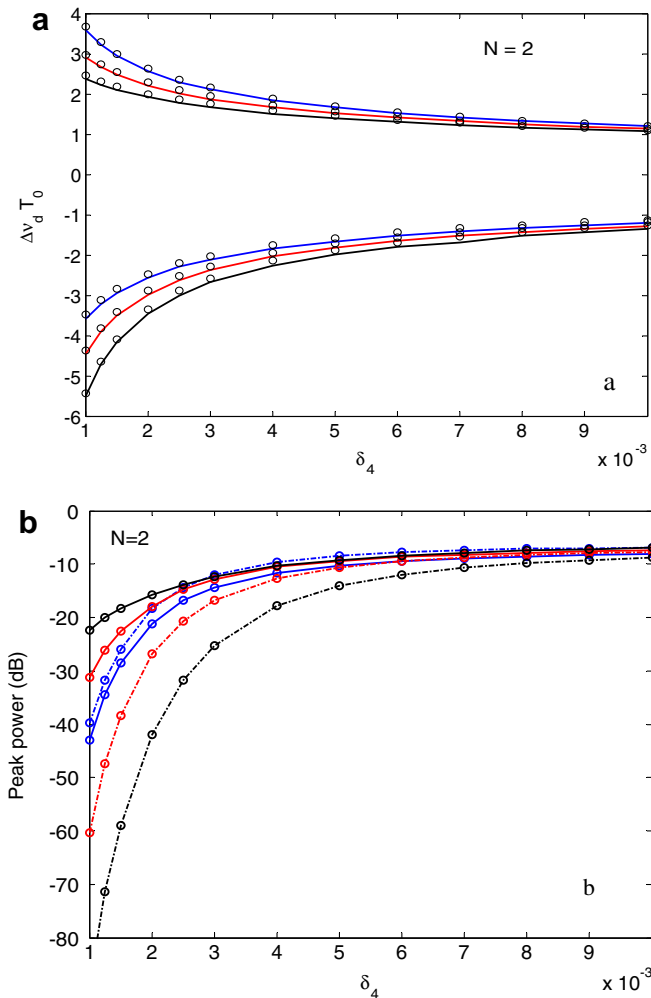
Fig. 3. (a) Frequencies and (b) relative peak powers of the red and blue NSR peaks plotted as a function of δ_4 for three values of δ_3. The blue, red and black lines are for $\delta_3 = 0$, $\delta_3 = 0.01$ and $\delta_3 = 0.02$, respectively. In figure (a) the open circles show the numerical values and the solid lines represent the analytical prediction. In figure (b) the solid lines and the dot-dashed lines represent the peak powers of the red and blue NSR peaks, respectively. (For interpretation of the references to colour in this figure legend, the reader is referred to the web version of this article.)
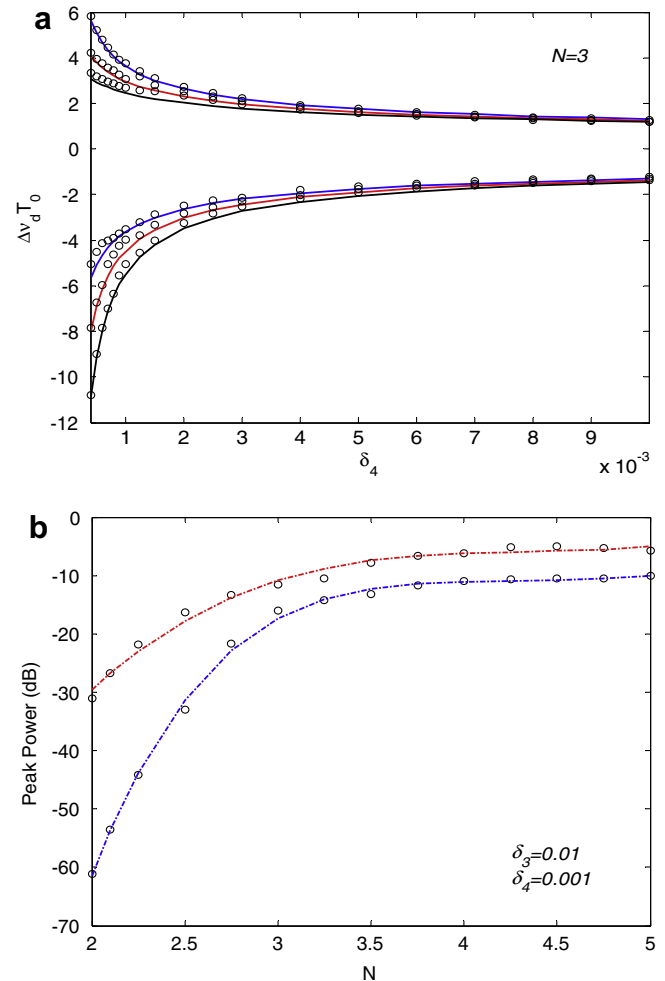
Fig. 4. (a) Frequency of relative peak powers of the red and blue NSR peaks plotted as a function of δ_4 for $N = 3$ with three values of δ_3. The blue, red and black lines are for $\delta_3 = 0$, $\delta_3 = 0.01$ and $\delta_3 = 0.02$, respectively. The open circles show the numerical values and the solid lines represent the analytical prediction. In figure (b) the evolution of the peak powers is shown qualitatively for different soliton order. The open circles stand for the numerical data where as the red and blue dotted curves represent the average evolution of blue and red peak, respectively. (For interpretation of the references to colour in this figure legend, the reader is referred to the web version of this article.)

Fig. 5. Same as in Fig. 3 except that the ratio of δ_3 and δ_4 is fixed at 10.

ultrashort optical pulses are used to excite them. We study, both analytically and numerically, how the radiation emitted by solitons in the form of dispersive waves is affected by the FOD. We include the effects of TOD as well because both types of dispersions are present simultaneously in most practical cases. Moreover, we include the impact of IPRS because this process is essential for supercontinuum generation. Our results show that two dispersive wave sidebands appear in the output spectrum on opposite sides of the input spectrum. Their frequencies are set by the relative magnitudes of the third- and fourth-order dispersion parameters as well as by the order of the soliton, but they are not affected much by the IPRS process. A well defined phase-matching condition can predict the exact location of radiation peaks in frequency domain. The relative amplitudes of conjugate sidebands are not equal because of the asymmetry induced by the third-order dispersion. Although the amplitude of both spectral components saturate eventually, the relative power level associated with the high-frequency component (for $\delta_3 > 0$) on the blue side of the launched wavelength may exceed 10% of the launched power under suitable conditions. In a fiber with $\delta_3 < 0$ it is the low-frequency component on the red side of the launched wavelength that has such high power levels. The effects of FOD have not attracted much attention so far except for a recent experimental demonstration of the two NSR spectral components. Our results reveal several interesting features that should be of relevance for applications requiring an ultrabroadband optical source.

Acknowledgements

References

[1] G.P. Agrawal, Nonlinear Fiber Optics, fourth ed., Academic Press, Boston, 2007.
[2] A. Hasegawa, M. Matsumoto, Optical Solitons in Fibers, Springer, New York, 2002.
[3] J.P. Gordon, L.F. Mollenauer, Solitons in Optical Fibers, Fundamentals and Applications, Academic Press, Boston, 2006.
[4] P.K.A. Wai, C.R. Menyuk, Y.C. Lee, H.H. Chen, Opt. Lett. 11 (1986) 464.
[5] A.V. Husakou, J. Herrmann, Phys. Rev. Lett. 87 (2001) 203901.
[6] K.M. Hilligsøe, H.N. Paulsen, J. Thøgersen, S.R. Keiding, J.J. Larsen, J. Opt. Soc. Am. B 20 (2003) 1887.
[7] I. Cristiani, R. Tediosi, L. Tartara, V. Degiorgio, Opt. Exp. 12 (2004) 124.
[8] D.R. Austin, C.M. Sterke, B.J. Eggleton, T.G. Brown, Opt. Exp. 14 (2006) 11997.
[9] J.M. Dudley, G. Genty, S. Coen, Rev. Mod. Phys. 78 (2006) 1135.
[10] P.K.A. Wai, H.H. Chen, Y.C. Lee, Phys. Rev. A 41 (1990) 426.
[11] J.N. Elgin, Phys. Rev. A 47 (1993) 4331.
[12] V.I. Karpman, Phys. Rev. E 47 (1993) 2073.
[13] N. Akhmediev, M. Karlsson, Phys. Rev. A 51 (1995) 2602.
[14] S. Roy, S. Bhadra, G.P. Agrawal, Phys. Rev. A 79 (2009) 023824.
[15] F. Benabid, F. Biancalana, P.S. Light, F. Couny, A. Luiten, P.J. Roberts, J. Peng, A.V. Sokolov, Opt. Lett. 33 (2008) 2680.
[16] E.N. Tsoy, C.M. de Sterke, Phys. Rev. A 76 (2007) 043804.
[17] F. Poletti, P. Horak, D.J. Richardson, IEEE Photon. Technol. Lett. 20 (2008) 1414.
[18] B. Kibler, P.A. Lacourt, F. Courvoisier, J.M. Dudley, IEEE Electron. Lett. 43 (2007) 967.
[19] T. Schreiber, T.V. Andersen, D. Schimpf, J. Limpert, A. Tunnermann, Opt. Exp. 13 (2005) 9556.
[20] M.H. Frosz, P. Falk, O. Bang, Opt. Exp. 13 (2005) 6181.
[21] A. Mussot, M. Beaugeois, M. Bouazaoui, T. Sylvestre, Opt. Exp. 15 (2007) 11553.
[22] Q. Lin, G.P. Agrawal, Opt. Lett. 31 (2006) 3086.

between the analytical and numerical results as expected Eq. (3). Moreover, we also estimate the amplitude growth of the NSR with increasing soliton order N. As seen in Fig. 4b, the amplitude of radiation grows rapidly with N and eventually saturates.

As we discussed earlier, the competition between the TOD and FOD effects is an important feature of our work, and both perturbations contribute when the ratio of δ_3 and δ_4 is fixed at 10. Fig. 5a shows the frequencies of the two NSR peaks as a function of δ_4, with the ratio $\delta_3/\delta_4 = 10$. The corresponding peak amplitudes are plotted in Fig. 5b. The most noteworthy feature in Fig. 5b is that, although the amplitudes tend to saturate with increasing values of δ_4, there is a significant difference in the two saturated values. For the ratio $\delta_3/\delta_4 = 10$, the blue peak saturates at a level around -8 dB whereas the red peak acquires its maximum amplitude around -40 dB, and this amplitude gradually decreases with a further increase in δ_4. The reason is that for a fixed ratio of δ_3 and δ_4, the value of δ_3 increases with increasing δ_4, and eventually the effects of TOD begin to dominate over those of FOD.

5. Conclusions

Solitons forming inside optical fibers are perturbed by several higher-order dispersive and nonlinear effects, especially when